Efficiency of the benthic filter: Biological control of the emission of dissolved methane from sediments containing shallow gas hydrates at Hydrate Ridge

S. Sommer,[1] O. Pfannkuche,[1] P. Linke,[1] R. Luff,[2] J. Greinert,[1] M. Drews,[1] S. Gubsch,[3] M. Pieper,[1] M. Poser,[4] and T. Viergutz[5]

Received 20 October 2004; revised 23 November 2005; accepted 3 February 2006; published 20 June 2006.

[1] In marine sedimentary environments, microbial methanotrophy represents an important sink for methane before it leaves the seafloor and enters the water column. Using benthic observatories in conjunction with numerical modeling of pore water gradients, we investigated seabed methane emission rates at cold seep sites with underlying gas hydrates at Hydrate Ridge, Cascadia margin. Measurements were conducted at three characteristic sites which have variable fluid flow and sulfide flux and sustain distinct chemosynthetic communities. In sediments covered with microbial mats of *Beggiatoa,* seabed methane efflux ranges from 1.9 to 11.5 mmol m^{-2} d^{-1}. At these sites of relatively high advective flow, total oxygen uptake was very fast, yielding rates of up to 53.4 mmol m^{-2} d^{-1}. In sediments populated by colonies with clams of the genus *Calyptogena* and characterized by low advective flow, seabed methane emission was 0.6 mmol m^{-2} d^{-1}, whereas average total oxygen uptake amounted to only 3.7 mmol m^{-2} d^{-1}. The efficiency of methane consumption at microbial mat and clam field sites was 66 and 83%, respectively. Our measurements indicate a high potential capacity of aerobic methane oxidation in the benthic boundary layer. This layer potentially restrains seabed methane emission when anaerobic methane oxidation in the sediment becomes saturated or when methane is bypassing the sediment matrix along fractures and channels.

Citation: Sommer, S., O. Pfannkuche, P. Linke, R. Luff, J. Greinert, M. Drews, S. Gubsch, M. Pieper, M. Poser, and T. Viergutz (2006), Efficiency of the benthic filter: Biological control of the emission of dissolved methane from sediments containing shallow gas hydrates at Hydrate Ridge, *Global Biogeochem. Cycles*, *20*, GB2019, doi:10.1029/2004GB002389.

1. Introduction

[2] Marine gas hydrate deposits represent a significant reservoir and a potential source for methane carbon to the ocean. The global amount of methane carbon bound in submarine gas hydrates, mostly common in productive continental margin sediments, is estimated to be in the range of 1 to 5 $\times$ 10^{15} m^3 ($\sim$500–2500 Gt of methane carbon) [*Milkov*, 2004]. During destabilization of shallow gas hydrates under increasing temperature and/or lowered pressure conditions, enormous amounts of methane can be released. There is evidence that during the Quaternary ($\sim$60 kyr ago) massive release of methane is related to climate oscillations with concurrent warm deepwater conditions in the North Pacific [*Kennett et al.*, 2000]. For the Late Paleocene ($\sim$55 myr ago) a distinct increase of the deepwater temperature of about 4° to 8°C is postulated to have triggered rapid destabilization of gas hydrates releasing massive amounts of methane from the seafloor [cf. *Dickens*, 1999]. These findings rise questions about the fate of methane once released from decomposing gas hydrates and the source strength of sediments containing gas hydrates.

[3] Once methane is released, it is transported within the sediment column by molecular diffusion and advection to the sediment water interface [*Linke et al.*, 1994; *Luff and Wallmann*, 2003]. If the pore water velocity increases (>90 cm yr^{-1}) methane leaves the sediment, bypassing the sediment matrix, along fractures and channels, either dissolved in the pore water or in form of gas bubbles [*Luff et al.*, 2004]. Increased water release during gas hydrate decomposition enhances advective methane transport through the sediment matrix and bubble ebullition eventu-

[1]Leibniz-Institut für Meereswissenschaften an der Universität Kiel (IFM-GEOMAR), Kiel, Germany.
[2]Bundesamt für Strahlenschutz Messknotennetz Rendsburg, Rendsburg, Germany.
[3]Meerestechnik I, Technische Universität Hamburg-Harburg, Hamburg, Germany.
[4]Institut für Experimentelle und Angewandte Physik, Universität Kiel, Kiel, Germany.
[5]Meerestechnik Bremen GmbH, Bremen, Germany.

0886-6236/06/2004GB002389

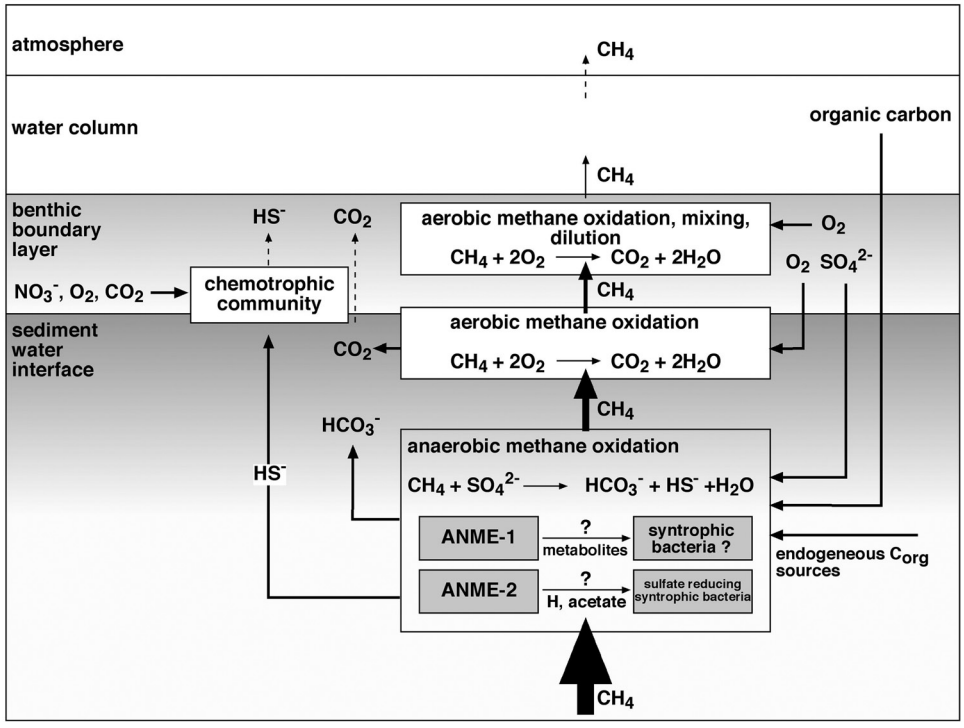

Figure 1. Scheme of the benthic filter for methane (see text for explanation).

ally destabilizes the sediment matrix and might lead to slope failures and sediment sliding on the continental slopes. During these processes, when the bulk density of the sediment becomes greatly reduced and its porosity increases, large pieces of gas hydrates may detach from the seafloor and rapidly ascend to the water surface. This process has been recognized as an efficient transport mechanism of methane from the seabed to the atmosphere [*Suess et al.*, 2001], bypassing all filter mechanisms in the sediment and water column.

[4] In sedimentary environments dominated by slow advective pore water transport and diffusion but also in freshwater systems and soils [cf. *Reeburgh*, 2003] microbial methanotrophy has been early recognized as an important control mechanism for methane flux [*Reeburgh et al.*, 1993; *Valentine et al.*, 2001]. These microbial processes embedded within a complex network of biogeochemical reactions control the methane emission across the sediment water boundary layer (Figure 1).

[5] Aerobic oxidation of methane (AEOM)

$$CH_4 + 2O_2 \rightarrow CO_2 + 2H_2O \quad (1)$$

and anaerobic oxidation of methane (AOM)

$$CH_4 + SO_2^{2-} \rightarrow HCO_3^- + HS^- + H_2O \quad (2)$$

are the major pathways of microbial methane consumption, releasing CO_2 and sulfide into the pore water. Aerobic methanotrophs can be found in virtually all oxic habitats containing methane [*Heyer*, 1990; *Reeburgh*, 1996]. On the basis of methane distributions in anoxic sediments, AOM was postulated by *Barnes and Goldberg* [1976], *Reeburgh* [1976], and *Martens and Berner* [1977]. On the basis of thermodynamic modeling, *Hoehler et al.* [1994] suggested that methanogenic archaea closely coupled to sulfate-reducing bacteria could gain energy from AOM. Visual evidence of an association between methanogenic archaea and sulfate-reducing bacteria was provided by the FISH studies of *Boetius et al.* [2000] which showed aggregations of both cell types in gas hydrate-containing sediments at Hydrate Ridge. So far three lineages of archea (ANME-1, ANME-2, ANME-3) have been identified mediating methane consumption in anoxic sediments [cf. *Orphan et al.*, 2001a, 2001b; *Valentine and Reeburgh*, 2000; *Valentine*, 2002; *Hinrichs and Boetius*, 2002; *Knittel et al.*, 2003]. At sites with shallow gas hydrates and high AOM turnover, the released sulfide sustains specifically adapted chemosynthetic microbial, meiobenthic, and macrobenthic communities [cf. *Olu et al.*, 1997; *Fisher et al.*, 2000; *Sahling et al.*, 2002; *Levin et al.*, 2003; *MacDonald et al.*, 2003; *Sommer et al.*, 2003; *Knittel et al.*, 2003].

[6] Because of a limited access to appropriate in situ technology, the influence of microbial methane turnover on seabed methane emission rates has been hardly resolved. For the cold vent sites at Hydrate Ridge characterized by sediments containing shallow gas hydrates and various fluid flow velocities of pore waters from below, great inconsistency exists between emission rates measured in situ [*Torres et al.*, 2002] and methane fluxes derived from numerical modeling of pore water gradients [*Luff and Wallmann*,

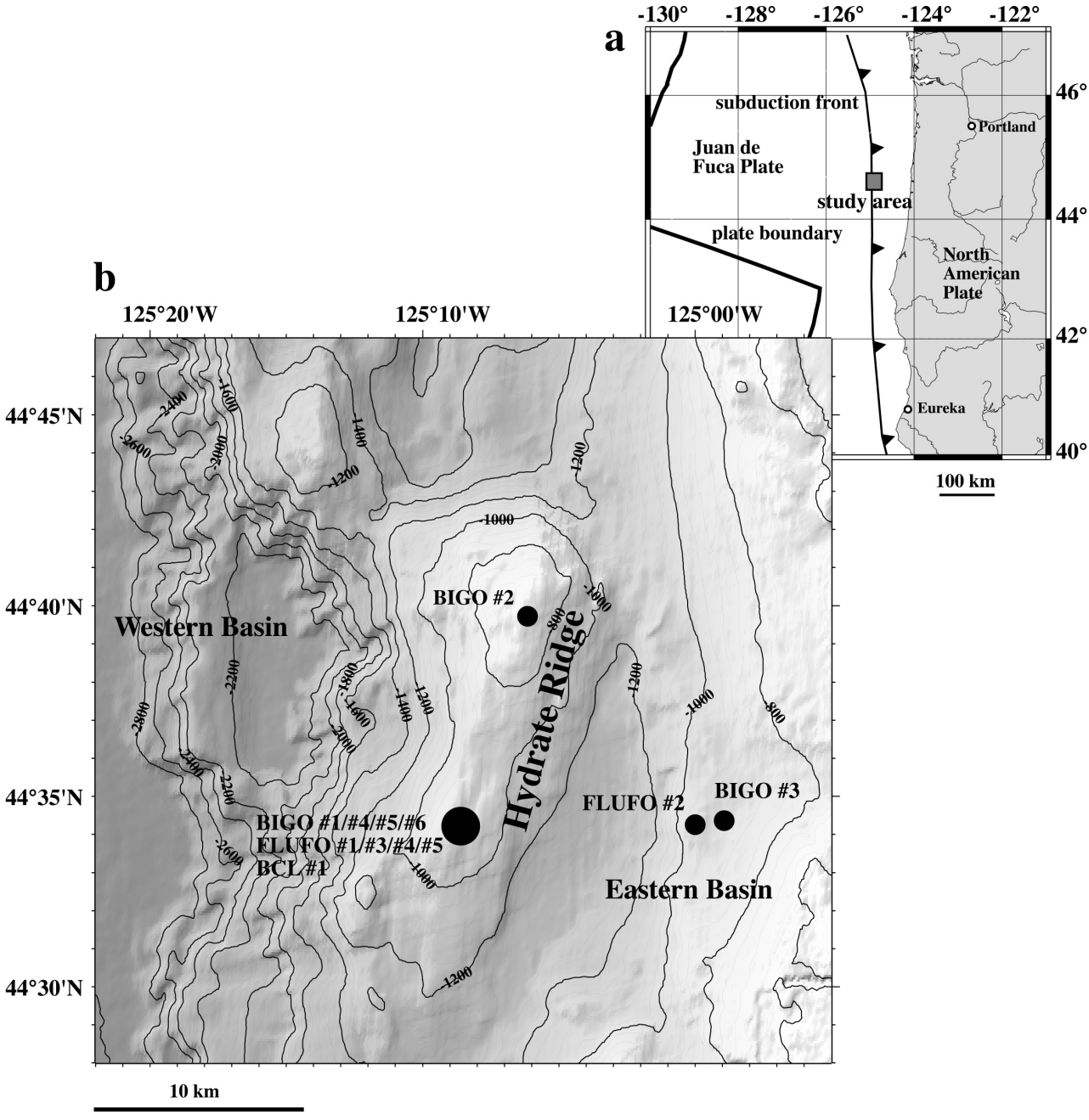

Figure 2. Sites sampled at Hydrate Ridge, Cascadia subduction zone, off the coast of Oregon. (a) Overview; (b) Hydrate Ridge and adjoint western and eastern basins.

2003; *Treude et al.*, 2003]. While pore water data only mirror the slow transport through the sediment matrix, in situ measurements revealed fast advective fluid flow at distinct spots, bypassing the methane consuming microbial communities [*Luff et al.*, 2004]. Differences of up to three orders of magnitude have been found due to the different approaches. Moreover, extreme temporal and lateral inhomogeneities exist at this site, which makes it difficult to estimate the overall methane flux into the bottom water. This study provides for the first time in situ measurements of seafloor methane emission rates under controlled oxygen and current conditions.

2. Materials and Methods

2.1. Study Area and Sediment Sampling

[7] During cruise 165-1 of RV *Sonne* in July/August 2002 in situ flux measurements of oxygen, methane and partly nitrate and pore water determinations were conducted at the northern and southern summit of Hydrate Ridge as well as in the eastern basin adjoint to Hydrate Ridge (Figure 2 and

Table 1. Station Data of Cruise SO 165/1

Site	Habitat	Date	Position	Depth, m	$t_{inc.}$[a] h
BIGO 1	control	14 Jul 2002	44° 33.9800′N, 125° 08.3800′W	832	16.0
BIGO 2	clams	18 Jul 2002	44° 39.8670′N, 125° 06.1150′W	605	32.4
BIGO 3	mat	21 Jul 2002	44° 34.2893′N, 124° 59.8887′W	883	36.4
BIGO 4	mat	26 Jul 2002	44° 34.2303′N, 125° 08.7705′W	778	20.5
BIGO 5	clams	29 Jul 2002	44° 34.2105′N, 125° 08.7800′W	777	20.5
BIGO 6	mat	31 Jul 2002	44° 34.2401′N, 125° 08.7734′W	782	16.7
FLUFO 1	control	15 Jul 2002	44° 34.0000′N, 125° 08.8600′W	779	43.5
FLUFO 2	mat	20 Jul 2002	44° 33.3060′N, 125° 59.8640′W	880	42.0
FLUFO 3	mat	23 Jul 2002	44° 34.2270′N, 125° 08.7920′W	779	64.0
FLUFO 4	clam	28 Jul 2002	44° 34.1867′N, 125° 08.7730′W	777	55.0
FLUFO 5	mat	30 Jul 2002	44° 34.2044′N, 125° 08.8183′W	777	37.7

[a]Here $t_{inc.}$ indicates the incubation time of chamber measurements.

Table 1). Hydrate Ridge belongs to the accretionary complex of the Cascadia convergent margin, where extensive vent communities [*Suess et al.*, 1985; *Boetius et al.*, 2000; *Sahling et al.*, 2002], methane hydrate exposures and authigenic carbonates have been discovered [*Greinert et al.*, 2001]. In this region, shallow gas hydrates occur directly on or a few centimeters below the sediment surface. The gas hydrate affected sites can be divided into three characteristic habitats along a gradient of sulfide flux (see equation (2)) which were sampled by TV-guided observatories. Dense mats of the sulfide-oxidizing bacteria *Beggiatoa* sp. (stations BIGO 3, 4, 6, FLUFO 2, 3, 5) occur directly above gas hydrates in association with high sulfide fluxes of up to 63 ± 36 mmol m^{-2} d^{-1} [*Sahling et al.*, 2002]. At reduced sulfide fluxes of 18 ± 6.5 mmol m^{-2} d^{-1} the outer rim of the bacterial mats becomes extensively populated by vesicomyid clams of the genus *Calyptogena* sp. (stations BIGO 2, 5, FLUFO 5). Sediments with low sulfide fluxes are populated by the burrowing solemyid bivalve mollusc *Acharax* sp. Reference measurements (stations BIGO 1, FLUFO 1) were conducted at locations without gas hydrates on the southern summit of Hydrate Ridge. At these sites no particular vent fauna was present and the sediment contained no dissolved sulfide in the upper 10 cm.

2.2. Benthic Observatories

[8] In situ flux measurements were conducted using the Biogeochemical Observatory (BIGO; Figure 3) and the Fluid-Flux Observatory (FLUFO). The technical design of BIGO and FLUFO is based on the GEOMAR Benthic Chamber Lander [*Witte and Pfannkuche*, 2000; *Linke et al.*, 2005]. The basic frame of these observatories consists of a titanium tripod that carries 21 Benthos glass spheres for buoyancy and a ballast weight attached to each leg by release toggles. Release of ballast is controlled by two acoustic release units. A radio beacon and strobe light assist in location and recovery at the surface. An ARGOS system is used to track the observatory in case of a premature release. Each of the observatories contained two large circular chambers (internal diameter 28.8 cm), providing a sediment area of 651.4 cm^2. This is an appropriate size for sediment subsampling and minimizing smearing and disturbance effects on the inner sediment core when the chamber is driven into the sediment. As shown by *Glud and Blackburn* [2002] flux measurements in larger chambers are less susceptible for errors when calculating area budgets and fluxes.

[9] A TV-guided launching system allowed smooth placement of the observatories at selected sites on the seafloor. Two hours after the observatories had been released from the launcher and placed on the seafloor the chambers were slowly driven into the sediment (~30 cm h^{-1}). Average water volume enclosed by benthic chambers during deployment of BIGO was 11.2 l and of FLUFO 20.1 l. Each chamber is an autonomous module with its own control unit and power supply. During each deployment seven sequential water samples were collected from the enclosed water column with syringe samplers attached to the chamber. The volume (~46 ml) drawn by each syringe was replaced by ambient bottom water. All chambers were equipped with two backpressure valves. When the chambers were driven into the sediment excess water can leave and overpressure inside the chamber is avoided. These valves further allow unimpeded fluid flow across the sediment water interface at seep sites. During BIGO 5/6 deployments additional water samples were taken from the bottom water outside the chambers at a height of about 30–40 cm above the seafloor. Duration of the flux measurements from first-to-last syringe sampling varied between 16 and 64 hours. Except for FLUFO deployments, the incubated sediments were retrieved after the in situ measurements for on board analyses of pore water by closing the chamber with a particular shutter mechanism. Once the shutter was closed, the chambers were slowly heaved out of the sediment and the observatory was ready for recovery.

[10] In order to record long-term variability of benthic fluxes and turnover in semiclosed chamber systems it is of crucial importance to maintain the oxygen supply at natural levels and to avoid severe oxygen depletion which would cause stress responses of the enclosed organisms and alteration of the vertical geochemical concentration profiles. Thus a gas exchange system similar to the ''gilled'' benthic chamber as described by *Morse et al.* [1999] has been designed to compensate for the total oxygen consumption of the enclosed bottom water and the sediment (Figure 4). This system ensures transfer of dissolved oxygen from a reservoir (volume 31.6 l) into the benthic chamber to keep the oxygen concentration constant. Prior to the deployment this reservoir was filled with filtered (0.4 μm) oxygen-saturated bottom water. The chamber water circuit and the water circuit of the reservoir is separated by silicone membranes

Figure 3. Biogeochemical observatory (BIGO) with launcher on top ready for video-guided deployment.

allowing diffusive exchange of oxygen, methane, and other gases. The gas exchange system contains a stack of five silicone membranes each 125 μm thick, providing a total gas exchange area of 392.7 cm^2. During the in situ measurements BIGO was equipped with one "exchange chamber" with and one "control chamber" without the gas exchange system. Although FLUFO has originally been designed for a different type of flux studies, during this investigation its chambers were used in the same mode as the "control chamber" deployed in BIGO.

[11] Fluxes of solutes across the sediment water interface are highly susceptible to alterations of shear stress pattern at the sediment surface [*Thomsen and Gust*, 2000]. Thus all chambers contained a system mimicking the external shear stress on the enclosed sediment surface [*Gust*, 1990]. The operation principle of this system is based on an internal fluid transport system, which is simultaneously driven by a rotation disc above the sediment and a pump, which removes the fluid from the center of the experimentation area. By operating the disc (diameter: 15 cm with a skirt of 6 cm) and pump at calibrated settings, a spatially homogeneous shear stress pattern is generated at the sediment surface [*Tengberg et al.*, 2004]. For the in situ measurements the internal shear stress was coupled on the external flow regime by regulating both rotation velocity and pump rate on an external flow sensor (Savonius rotor) signal. To assure adequate mixing of the enclosed water body during periods of slow bottom currents (<5 cm s^{-1}), the rotation velocity of the disc was set to a minimum of 9 rpm.

2.3. Analytical Techniques

2.3.1. Water Samples

[12] Oxygen concentrations of the syringe samples were fixed immediately after retrieval of the observatories. Within 12 hours the oxygen content of water samples was determined by automated Winkler titration [*Grasshoff et al.*, 1983]. Figure 5 displays a typical time course of the oxygen concentration in the chambers, reservoir, and the bottom

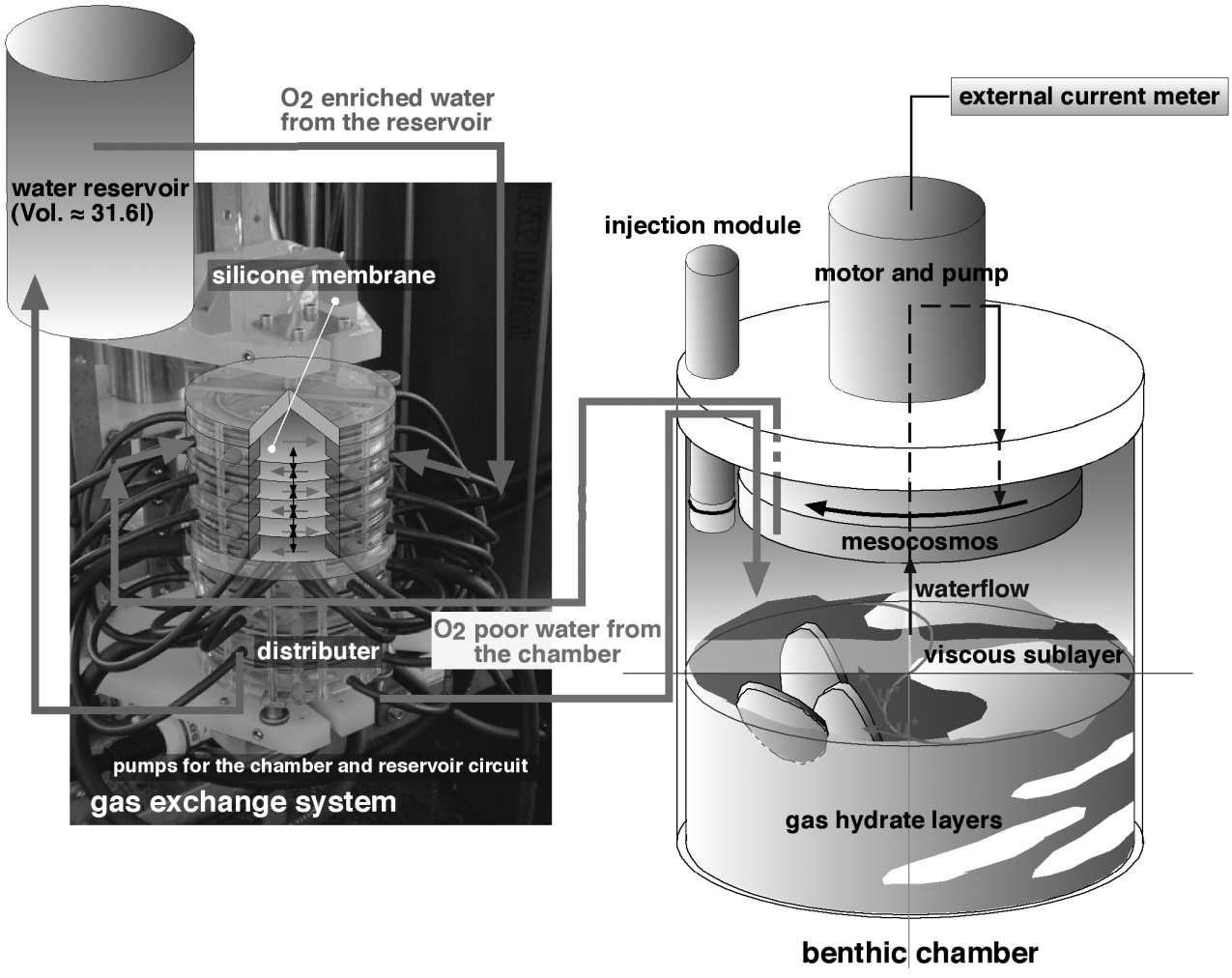

Figure 4. Gas exchange system connected with the benthic chamber. The chamber water circle (O_2-poor water) is separated from the reservoir circle (O_2-enriched water) by silicone membranes, which allow exchange of methane and oxygen.

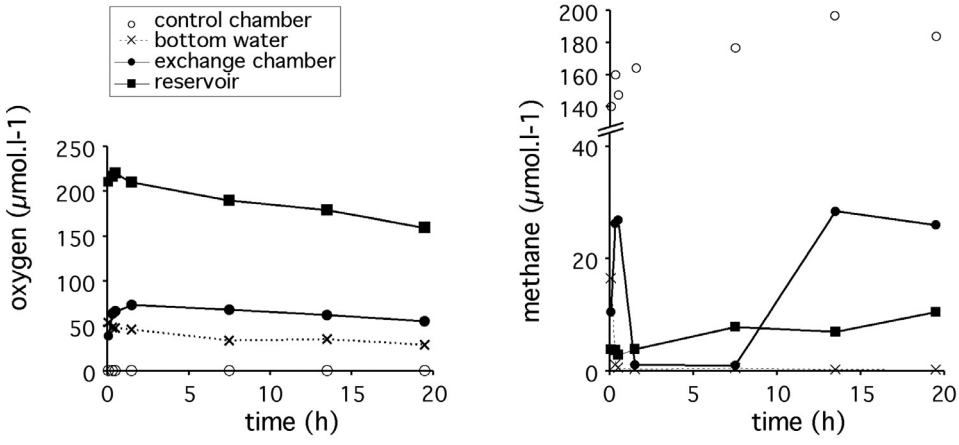

Figure 5. Time course of oxygen and methane in the control chamber not equipped with a gas exchange system, the exchange chamber equipped with the gas exchange system, the reservoir, and the bottom water at a microbial mat site (BIGO 4).

water (BIGO 4). Total oxygen consumption was calculated using the linear decrease of the oxygen concentration with time.

[13] Methane concentrations were determined by "head space" analysis modified after *Linke et al.* [2005]. Immediately after retrieval of the observatories, 10 mL of the syringe water samples were carefully transferred into septum stoppered 24 mL glass vials which contained 10 mL saturated sodium chloride solution. The volume ratio of sample to headspace was 10/4. Within 24 h the methane concentration in the headspace was determined using a Shimadzu GC14A gas chromatograph fitted with a flame ionization detector and a 4 m 1/8′ Poraplot Q (mesh 50/80) packed column. Prior to the measurements the samples were equilibrated for 2 h in a shaking table.

[14] In order to calculate the methane flux out of the sediments from the concentration changes in the samples, two effects caused by the benthic chamber have to be considered. Although the chambers were driven very slowly into the sediment, during the initial phase (up to 1.5 h) of the measurement leakage of methane from the disturbed sediment can be observed. Whereas in the natural environment methane emitted from the sediment is continuously swept away and diluted by bottom water currents, methane concentration in the enclosed water body increases with time. Thus the concentration gradient between the sediment and the enclosed water body decreases, which reduces the diffusive transport and affects methane emission in the chamber. This rise of the methane concentration can be described by an exponential function ($C = a(1 - e^{-lt}) + b$, where C is methane concentration (μmol L^{-1}), t is time (h), and a, b, and l are fitting parameter). Methane flux was calculated after the initial phase of the experiment using the first derivative of the exponential function, which was fitted to the time course of the methane concentrations.

[15] Nitrate concentration in the water samples were measured using standard photometric procedures [*Grasshoff et al.*, 1983]. Nitrite uptake was calculated using the linear decrease of the nitrate concentration with time.

2.3.2. Pore Water Chemistry

[16] After recovery, the retrieved sediments were subsampled and sediment cores were rapidly transferred to the onboard laboratory, which was cooled to 4°C. The cores were segmented into 1 cm slices for pressure filtration. Pore water was squeezed from the sediment through 0.2 μm cellulose acetate membrane filters at up to 3 bar pressure applying argon gas with a mechanical polypropylene press. Pore waters were analyzed on board for dissolved nitrate, ammonia, and sulfide using standard photometric procedures [*Grasshoff et al.*, 1983; *Gieskes et al.*, 1991]. Total alkalinity was determined by pore water titration [*Ivanenkov and Lyakhin*, 1978]. The remaining pore waters were later analyzed in the home laboratory for dissolved sulfate and bromide. Detailed descriptions of the methods are available at http://www.ifm-geomar.de/index.php?id=mg_analytik&L =0.

2.3.3. Numerical Modeling

[17] The numerical transport reaction model Calcite, Carbon and Nutrient Diagenesis (C. CANDI) was applied to simulate the biogeochemical processes in the surface sediments at clam fields (BIGO 5) and sediments covered with bacterial mats (BIGO 4) as typical examples for these specific environments. This model is able to reproduce the benthic turnover at cold vent sites and therewith to determine the major biogeochemical processes in the sediment and the fluxes between sediment and bottom water [*Luff and Wallmann*, 2003]. The rates of the kinetically controlled redox reactions are formulated following *Van Cappellen and Wang* [1996] and *Boudreau* [1996]. Dissolution and precipitation rate laws for calcium carbonate were taken from *Hales and Emerson* [1997]. The equilibrium calculations for the simulations of the two BIGOs were performed using the alkalinity conservation approach as outlined by *Luff et al.* [2001]. The model considers the degradation of organic matter separated in two different fractions (2-G), the consumption of six terminal electron acceptors, 15 secondary redox reactions including anaerobic methane oxidation, acid-base equilibria, and carbonate dissolution and precipitation processes. Altogether the distribution of 19 species solid and solute (O_2, NO_3^-, MnO_2, Mn^{2+}, Fe(OH), Fe^{2+}, SO_4^{2-}, TPO_4, TNH_4, TCO_2, Alkalinity, CH_4, $POC_{reactive}$, $POC_{refractionary}$, TH_2S, TBOH, Ca^{2+}, $CaCO_{3(aragonite)}$, $CaCO_{3(calcite)}$), in the sediment and the pore water, evoked by advection, irrigation, molecular diffusion, bioturbation and chemical/biological reactions have been described with the model. The complete description of the model including the parameterization of bioturbation and bioirrigation, as well as the formulation of the chemical reactions, is given by *Boudreau* [1996].

[18] Critical values of kinetic constants, the unknown flow velocity, bioturbation and bioirrigation activities were determined by fitting the model to the available biogeochemical data set assuming steady state conditions. Measured bottom water concentrations (of, e.g., SO_2^{4-} and alkalinity) as well as measured particular organic carbon (POC) concentrations in the upper sediment layer have been used to define the upper boundary concentrations for the model. For the simulation of the upper 20 sediment centimeters, a vertical grid of 1500 cells has been used to resolve the high turnover, especially near the sediment surface.

3. Results

3.1. Reference Sites: In Situ Flux Measurements

[19] At reference sites the average total oxygen uptake was low at 2.1 ± 0.9 mmol m^{-2} d^{-1} (Table 2). Net methane efflux was not detected here, within the chambers methane concentrations remained stable over time at an average concentration of 0.04 ± 0.001 μmol L^{-1}. Background concentration of methane in this region is about 0.0015 μmol L^{-1} [*Heeschen et al.*, 2005]. Oxygen concentration of the bottom water was 56.7 μmol L^{-1}. Numerical modeling was not applied to pore water concentrations of these sites.

3.2. Clam Field Sites

3.2.1. In Situ Flux Measurements

[20] At clam field sites methane efflux under natural oxic conditions was 0.6 mmol m^{-2} d^{-1}. Oxygen concentrations inside the chamber never became less than 12.6 μmol L^{-1} (FLUFO 4). The total average oxygen uptake was about

Table 2. Average Fluxes and Turnover Rates Measured in Situ Under Natural Oxic Conditions and Derived From Numerical Modeling (BIGO 4/5) at Clam Fields and Microbial Mats in Comparison to Nearby Reference Sites[a]

	In Situ Measurements[b]		
Fluxes/Turnover	Control Site	Clam Bed	Microbial Mat
Total oxygen uptake	2.1 (1.5/3.2)	3.7 (2.0/5.1)	47.5 (38.0/53.4)
Total nitrate uptake	n.d.	4.8 (3.7/6.0)	4.6 (2.6/6.8)
Methane efflux	0	0.6 (0.2/1.1)	5.7 (1.9/11.5)
Aerobic oxidation of methane	0	n.d.	4.6

	Numerical Modeling[c]		
Fluxes/Turnover	Control Site	BIGO 5	BIGO 4
Methane flux (surface)	n.d.	0.0005	0.6
Methane flux (at 20 cm sediment depth)		3.6	16.5
Sulfide flux (surface) ($H2S + HS^-$)	n.d.	6.2	22.0
Sulfate flux	n.d.	3.6	15.0
AOM	n.d.	3.6	15.1
Fluid flow, cm yr^{-1}	n.d.	10	20
Bioirrigation, yr^{-1}	n.d.	20	0
Depth of irrigation, cm	n.d.	5	0

[a]All numbers except those for fluid flow, bioirrigation, and depth of irrigation are given in mmol m^{-2} d^{-1}. The numbers in parentheses denote minimum and maximum rates.
[b]Bottom water plus sediment.
[c]Sediment only.

1.7 times higher than at the control sites with a maximum uptake rate of 5.1 mmol m^{-2} d^{-1}. Average nitrate uptake was 4.8 mmol m^{-2} d^{-1}. Ambient bottom water concentrations of oxygen and methane above clam beds were 38.4 ± 4.9 and 0.09 ± 0.04 μmol L^{-1}, respectively.

3.2.2. Model Flux Calculations

[21] Model calculations have been applied to the measured pore water profiles of sulfate, sulfide and total alkalinity obtained with BIGO 5. The measurements from the chamber with and without the gas exchange system as well as the results from the simulation are shown in Figure 6. Biogeochemical turnover in the underlying sediment consumes about 1.4 mmol m^{-2} d^{-1} oxygen. The aerobic degradation of organic matter consumes about 0.57 mmol m^{-2} d^{-1} while the oxidation of reduced species near the sediment surface consumes the rest. Aerobic methane oxidation in the sediment does not play an important role (0.006 mmol m^{-2} d^{-1}). This turnover results in an oxygen

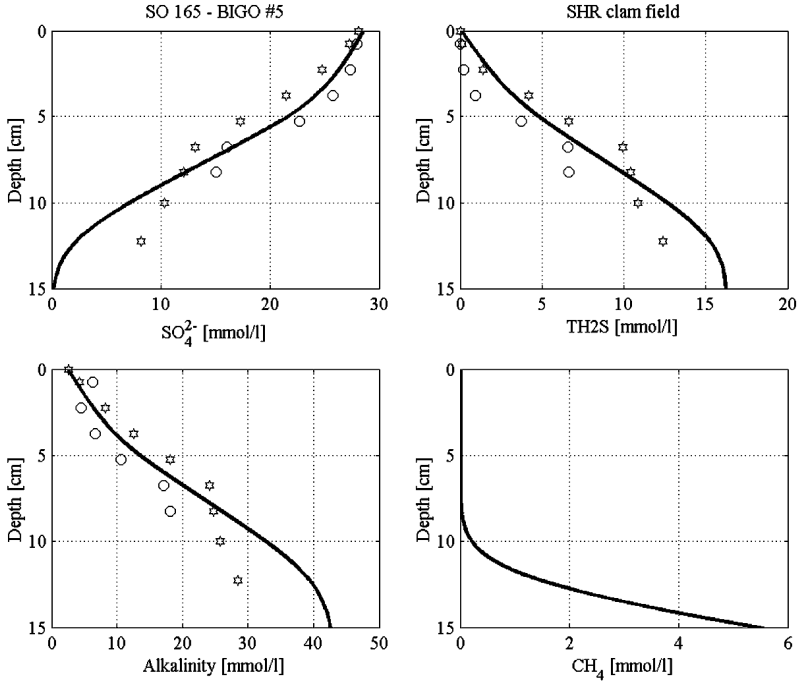

Figure 6. Simulated (solid line) and measured pore water profiles of sulfate, sulfide, alkalinity, and methane from the chamber with the gas exchange system (circles) and without the gas exchange system (stars) from BIGO 5. This core represents the biogeochemical situation below a clam field.

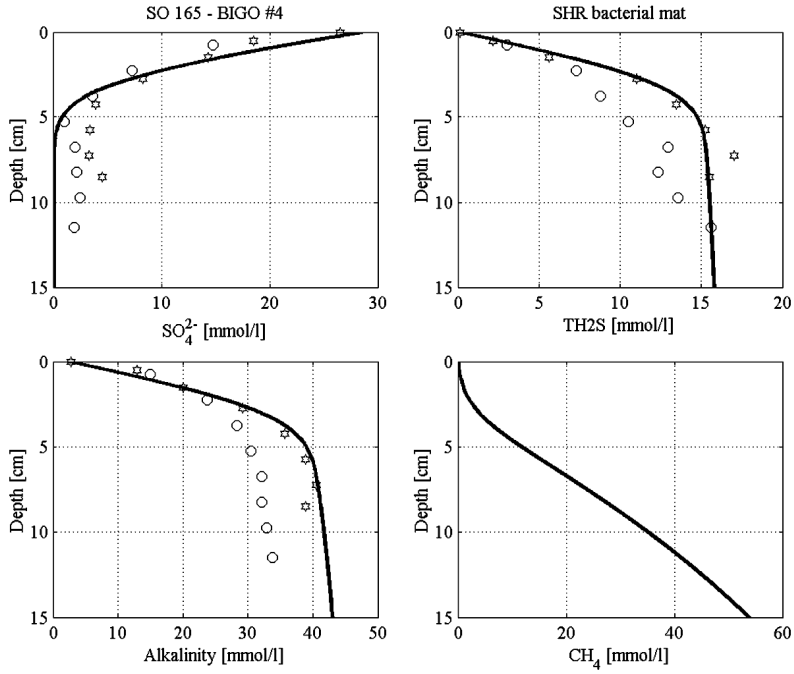

Figure 7. Simulated (solid line) and measured pore water profiles of sulfate, sulfide, alkalinity, and methane from the chamber with the gas exchange system (circles) and without the gas exchange system (stars) from BIGO 4. This core represents the biogeochemical situation below a microbial mat.

penetration depth of less than one millimeter. Pore water fluid flow from below has been resolved by the model to be 10 cm yr^{-1}. The lower concentration gradients near the sediment surface are an obvious indicator for bioirrigation activities. The best model fit could be obtained using a bioirrigation coefficient of 20 yr^{-1} and a depth of 5 cm. At this station sulfate penetrates down to a depth of about 20 cm, yielding an anaerobic oxidation rate of methane of 3.6 mmol m^{-2} d^{-1}. In this environment almost 100% of the methane reaching the sediment column at 20 cm depth is oxidized anaerobically within the sediment.

3.3. Microbial Mat Sites

3.3.1. In Situ Flux Measurements

[22] In comparison to the control and clam field sites, sediments covered with microbial mats are characterized by an extremely fast total oxygen uptake, yielding an average uptake of 47.5 mmol m^{-2} d^{-1}. This value is about 13 or 23 times higher than at clam field and control sites, respectively. In the "control chambers," where oxygen was not supplied during the measurements, oxygen was completely consumed within less than 20 min. Total oxygen uptake rates for these measurements were not calculated. Under these anoxic conditions average methane efflux was 117.0 mmol m^{-2} d^{-1} in contrast to 5.7 mmol m^{-2} d^{-1} under natural oxic conditions measured in the "exchange chamber". Under natural oxic conditions methane emission from these sediments was about 9 times higher than found at the clam field sediments. Average nitrate uptake of sediments covered with microbial mats under oxic conditions was 4.6 ± 1.7 mmol m^{-2} d^{-1}. Bottom water methane concentrations (0.34 ± 0.13) were slightly higher than those above clam fields, bottom water concentration of oxygen was 43.6 ± 8.1 μmol L^{-1}.

3.3.2. Model Flux Calculations

[23] In contrast to the numerical simulation of the clam fields, the concentration of oxygen and nitrate at the sediment surface below the bacterial mat has been set to zero. All oxygen and nitrate available in the bottom water is already consumed in the bacterial mat for organic matter remineralization and oxidation of reduced species from the sediments [*Sommer et al.*, 2002; *Luff and Wallmann*, 2003]. Microprofiling measurements by W. Ziebis (personal communication, 2002) further confirm the use of this approach. Thus the oxygen uptake of the sediment under the mat can be considered as negligible and the measured oxygen uptake of 47.5 mmol m^{-2} d^{-1} proceeds in the enclosed bottom water and the microbial mat. The simulation of the pore water concentrations (Figure 7) from BIGO 4 yields an anaerobic oxidation rate of methane of 15.1 mmol m^{-2} d^{-1} (Table 2). The sulfate flux to AOM ratio is 0.99 and like at the clam field site indicative for a tight coupling of methane turnover to sulfate reduction in sediments covered with microbial mats. The resulting sulfide flux corresponds to 22.0 mmol m^{-2} d^{-1} being 3.5 times higher than at the clam field. At this site fluid flow has been determined to a value of 20 cm yr^{-1}. A distinct methane flux of 0.6 mmol m^{-2} d^{-1} from the sediment into the bacterial mat has been found by the simulation.

Table 3. Comparison of Dissolved Methane Emission From the Seafloor at Hydrate Ridge Determined in Different Years by in Situ Measurements and Deduced From Numerical Modeling of Pore Water Profiles Using C. CANDI[a]

Date	Method	Reference	Clam Field	Microbial Mat	Reference
2002	in situ	not detectable	0.28	1.9	this study
2002	model	n.d.	0.016 [0]	0.28 [1–10]	this study
2000	model	n.d.	n.d.	0.6–4	*Treude et al.* [2003]
1999	model	n.d.	n.d.	0.027–134 [10–250]	*Luff and Wallmann* [2003]
1999	in situ	not detectable	<1 [2–10]	30–100 [10–250]	*Torres et al.* [2002], *Tyron et al.* [2002]

[a]Numbers in brackets denote advective pore water flow (cm yr^{-1}). Emission values are in mmol m^{-2} d^{-1}.

This flux represents only 3.6% of the methane entering the sediment column at 20 cm depth.

4. Discussion

4.1. Emission Rates of Dissolved Methane

[24] In situ measurements of emission rates of dissolved methane from gas hydrate containing sediments are very scarce because of limited availability of appropriate in situ technology. Deployment of lander systems is very labor intensive and time consuming, hence only a few single spot measurements are available. So far existing in situ measurements of seabed methane emission rates at Hydrate Ridge [*Torres et al.*, 2002] were in the range of 30 to 100 mmol m^{-2} d^{-1} in sediments covered with microbial mats and <1 mmol m^{-2} d^{-1} in clam field sediments. Compared to our in situ measurements at microbial mat sites these values are 5 to 18 fold higher whereas methane emissions from clam field sites are similar in both studies. The mismatch at microbial mats can be attributed to different velocities of the advective pore water flow where our model calculations revealed advective pore water velocities of about 20 cm yr^{-1} (Table 2). Three years prior to this study *Torres et al.* [2002] found at the southern summit of Hydrate Ridge advective flow rates of 10 to 250 cm yr^{-1} at microbial mat sites and 2 to 10 cm yr^{-1} at clam fields. Another factor contributing to this discrepancy of methane emission might be strong spatial and temporal variability. Table 3 summarizes methane emission at Hydrate Ridge from three different years determined by in situ methods and numerical modeling of pore water gradients. Methane efflux measurements are subject to methodological constraints of the lander systems. Even when the chambers are slowly driven into the sediment leakage of methane and other reduced pore water species takes place. Subsequent bacterial and chemical oxidation processes then lead to a fast depletion of the oxygen inventory inside the chamber, in effect the measurement becomes artificial not describing the natural environment. Such anoxic conditions can be assumed for the in situ measurements conducted by *Torres et al.* [2002] inducing elevated methane emission rates beyond the natural background. In chambers where steady oxygen supply is sustained, the increased methane concentration during the critical initial phase of the measurement is lowered by oxidation and conditions prior to the disturbance eventually will be approached. In these chambers extremely high methane consumption rates in the range of 6 to 42 μmol L^{-1} h^{-1} were measured during this initial phase. Although these numbers represent an artifact, they clearly indicate the strong potential capacity of the sediment water boundary layer to suppress seabed methane emission. Assuming that all of this methane consumption proceeds aerobically, an oxygen supply of 12 to 84 μmol L^{-1} h^{-1} is necessary during the initial measurement phase. In this case the oxygen content of the enclosed water body would be consumed within 0.5–3.7 h, which has been observed in chambers not equipped with the gas exchange system.

[25] Inconsistencies exist between the in situ methane emission rates and those calculated from pore water gradients. At the clam field sites a methane flux of 0.6 mmol m^{-2} d^{-1} has been measured by the observatories, while the numerical model predicts a flux of nearly zero (0.0005 mmol m^{-2} d^{-1}). At the microbial mat sites the fluxes determined in situ are 9.5 times higher than those determined by model calculations. These differences result from the different approaches. Benthic chambers enclose a natural mesoscale environment including sediment fractures and biogenic structures along which solutes and gases can easily escape. In contrast, the pore water concentrations used for the numerical simulation result from a squeezed sediment layer with a diameter of 10 cm, where all biogenic and geological sediment features are leveled out. Hence these data can only be described by diffusive and advective processes through the sediment matrix. Therefore the natural small-scale variability observed at cold vent sites explains the difference between the in situ and modeled fluxes.

[26] Because of the pronounced spatial heterogeneity of sediment lithology and faunal distribution, it is very difficult to extrapolate from these spot measurements to regional emission rates. Water column measurements across the vent sites of the southern Hydrate Ridge area (0.029 km^2) provided a regional methane flux estimate of 328 mmol m^{-2} d^{-1} [*Heeschen et al.*, 2005]. These measurements integrate the total methane flux of the summit dissolved in the pore water as well as in form of gas bubbles. Our in situ flux measurements, representing only 2% of this methane flux, emphasize the importance of gaseous methane emission for the water column carbon cycle.

4.2. Efficiency of the "Benthic Filter"

[27] So far only indirect estimates of the filter efficiency of the benthic system for methane exist. On the basis of methane emission rates of *Torres et al.* [2002] and ex situ determinations of the anaerobic methane oxidation *Treude et al.* [2003] provide an estimate of the filtering efficiency in the range of 50–90% for sediments covered with microbial

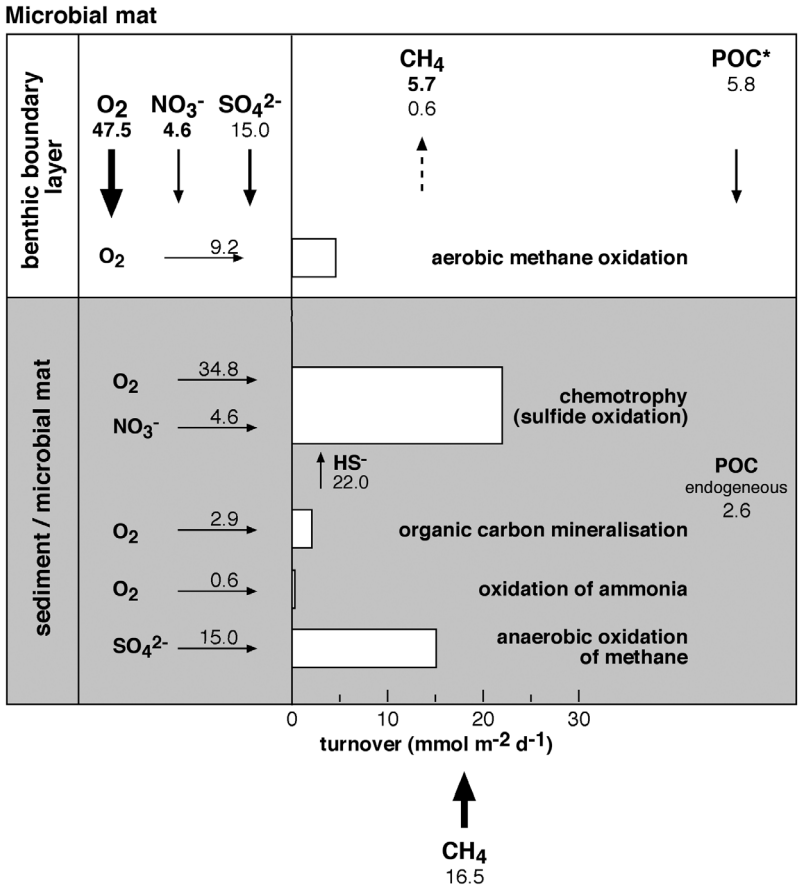

Figure 8. Fluxes of electron acceptors (O_2, NO_3^-, SO_4^{2-}) in relation to the turnover of methane, particulate organic matter, and microbial sulfide oxidation in sediments covered with microbial mats. Numbers in bold represent in situ measurements; those in plain text represent fluxes derived from modeling of pore water concentrations of sediments retrieved with BIGO 4, POC* flux is from *Sommer et al.* [2002]. See text for further explanations.

mats. *Boetius and Suess* [2004] postulate that less than 50% of the total methane escapes from sediments covered with bacterial mats and <15% from clam fields.

[28] Using the fluxes resolved from the model for the amount of methane, which enters at the bottom of the sediment column at 20 cm depth, and the modeled methane emission rates across the sediment water interface estimates of the efficiency of the benthic filter at the different sites can be derived. At clam field sites almost 100% of the incoming methane is consumed by methane oxidation. In sediments covered with bacterial mats the methane consuming efficiency is 96%. However, these calculations neglect bubble transport and are only valid as long as the pore water transport can be regarded as laminar through the sediment matrix. *Luff et al.* [2004] found that in environments with pore water velocities of >90 cm yr^{-1} the fluid flow bypasses the filter, breaks through the sediment surface, and delivers high amounts of methane into the bottom water. Using the respective in situ methane emission rates for these calculations, the methane consuming efficiency is 83% at clam field and 66% at microbial mat sites.

[29] Our measurements showed that under experimental anoxic conditions seabed methane efflux increased and the filtering efficiency of the benthic system became strongly reduced. This might be attributed to anoxic conditions switching off aerobic methane oxidation in the sediment water boundary layer. Since we did not measure aerobic and anaerobic oxidation of methane directly, a crude estimate of the aerobic methane oxidation can be obtained by mass balance calculation of the total oxygen turnover. Fluxes of major electron acceptors in relation to the turnover of methane and particulate organic matter in sediment covered with bacterial mats are summarized in Figure 8. On the basis of the stoichiometry for sulfide oxidation by oxygen

$$HS^- + 2O_2 + HCO_3^- \rightarrow SO_4^{2-} + CO_2 + 2H_2O \qquad (3)$$

and nitrate

$$NO_3^- + HS^- + CO_2 + 2H_2O \rightarrow SO_4^{2-}NH_4^+ + HCO_3^- \qquad (4)$$

and the assumption that half of the sulfide is oxidized by oxygen and the other half by nitrate, 73.3% (34.8 mmol

m^{-2} d^{-1}) of the total oxygen uptake and 100% of nitrate uptake is used to cover the sulfide flux for complete oxidation in microbial mats. The remaining 26.7% of the total oxygen uptake is used for aerobic oxidation of methane, mineralization of organic carbon, and oxidation of ammonia. On the basis of primary production and applying different export production models *Sommer et al.* [2002] estimated an allochthonous particulate carbon input of about 5.8 mmol m^{-2} d^{-1}. Chemoautotrophy in microbial mats and by free-living sulfide oxidizers represents an important endogenous carbon source which contributes to cover the carbon demand in this system. Employing the stoichiometric equations for the oxidation of sulfide with nitrate and oxygen [*Luff and Wallmann*, 2003] an endogeneous carbon input of about 2.6 mmol m^{-2} d^{-1} can be calculated providing a bulk POC availability of 8.4 mmol m^{-2} d^{-1}. Assuming that 25% of the available bulk organic carbon is mineralized aerobically [*Glud et al.*, 1999] and using a molar ratio between oxygen consumption and POC degradation of 1.4 [*Anderson and Sarmiento*, 1994], a total oxygen uptake of 2.9 mmol m^{-2} d^{-1} would be necessary for the aerobic degradation of this amount of organic matter, leaving 9.8 mmol m^{-2} d^{-1} for aerobic oxidation of methane and ammonia. Oxidation of ammonia released during mineralization of organic carbon (C/N ratio 6.6) consumes 0.6 mmol m^{-2} d^{-1} oxygen. Thus 9.2 mmol m^{-2} d^{-1} (19.4%) of the total oxygen uptake would be left for aerobic methane oxidation, corresponding to an aerobic methane consumption of 4.6 mmol m^{-2} d^{-1}. For the same investigation area, *Suess et al.* [1999] estimated that 60% of the oxygen is used for sulfide oxidation, 5% for the oxidation of ammonia and the rest (35%) for the oxidation of methane. For organically highly enriched shallow water sediments, *Schmaljohann* [1996] calculated that up to 28% of the total oxygen uptake is needed for aerobic methane oxidation.

[30] Oxygen penetration in sediments covered with microbial mats is only in the range of a few micrometers to millimeters (W. Ziebis, personal communication, 2002) so that methanotrophic bacteria dependent on oxygen supply might be located at the upper layer of microbial mats or most likely live attached to suspended particles in the sediment water boundary layer. Thus apart from the surface sediments the bottom water boundary layer might considerably contribute to the filtering efficiency of the benthic system.

[31] At the investigated clam field sites significance of aerobic methane oxidation cannot be assessed. Input of methane (3.6 mmol m^{-2} d^{-1}) was nearly in balance with the anaerobic oxidation of methane (4.1 mmol m^{-2} d^{-1}). Overall fluxes and turnover rates were distinctively lower than at the microbial mat sites. The sulfide flux drives a chemotrophic organic carbon production of 0.83 mmol m^{-2} d^{-1}, which is 3.1 times lower compared to the microbial mat sites. This endogeneous organic carbon production contributes only 12.5% to the bulk particulate organic carbon supply. To underline the low activity at this site the sulfide flux was 3.6 times lower than the average sulfide flux measured at Hydrate Ridge clam fields 3 years ago [*Sahling et al.*, 2002]. Average oxygen uptake is nearly similar to that determined for the reference site. To cover the demand for complete sulfide oxidation 100% of nitrate and 82.6% (3.05 mmol m^{-2} d^{-1}) of the total oxygen uptake is necessary. The remaining 17.4% of the total oxygen uptake are used for aerobic oxidation of methane, ammonia and organic carbon mineralization.

[32] Organic carbon cycling at the reference site is almost exclusively dependent on the allochthonous supply of organic carbon. Total oxygen uptake accounts for the mineralization of 1.5 mmol C m^{-2} d^{-1}, representing 23.9% of the bulk organic carbon flux [*Sommer et al.*, 2002], leaving 76.1% for anaerobic degradation and permanent burial. Total oxygen uptake rates at Hydrate Ridge are slightly higher than those found at the California continental slope (0.3–1.3 mmol m^{-2} d^{-1}) at depths from 790 to 1,190 m [cf. *Cai and Reimers*, 1995]. A predictive equation from these authors derived from measurements of the NE Pacific, expressing the total oxygen uptake as a function of bottom water concentration and organic carbon percentage of the surficial sediments, underestimated our measurements (0.39 mmol m^{-2} d^{-1}). The stations at which the predictive equation is based might not be representative for the reference sites investigated during this study. The investigated reference sites are likely to benefit from the export of organic carbon and increased methane concentrations which is produced at nearby chemotrophically dominated sites containing gas hydrates and enhanced carbon turnover in the sediment water boundary layer.

5. Conclusions

[33] Seafloor methane emission from Hydrate Ridge clam field and bacterial mat sites is presently very low. This is due to low advective pore water flow and efficient anaerobic methane consumption in the sediment column. At microbial mat sites where methane input from below is about 3 times higher than at clam fields we found strong indications that aerobic methane oxidation further controls the methane efflux. Aerobic methanotrophy takes place down to a threshold oxygen concentration of about 6.3 μmol L^{-1} [*Heyer*, 1990]. Thus this microbial process might still efficiently take place in oxic surface sediment layers of clam fields and to a minor extent in microbial mats. We assume that this process predominantly occurs in the bottom water layer close to the sediment surface where bacteria live attached to suspended particles or in detrital aggregates. Although measured under artificial conditions extremely high methane consumption rates in this layer point toward a strong potential capacity of the sediment water boundary layer to suppress seabed methane emission when the anaerobic methane oxidation in the sediment becomes saturated or when methane is bypassing the sediment matrix along fractures or channels. Although the investigated sites at Hydrate Ridge are under the present environmental conditions in a quiescent state, there are implications that under altered environmental conditions such as enhanced surface water productivity and warming of bottom water enhancing overall oxygen uptake in the sediment water boundary layer the benthic filter might lose its efficiency. In effect, high concentrations of methane

might be injected into the water column where it will be oxidized aerobically with a negative feedback on the overall oxygen inventory of the water masses [*Kennett et al.*, 2000; *Valentine et al.*, 2001; *Hinrichs et al.*, 2003]. *Joos et al.* [2003] predict a 4 to 7% decline of dissolved oxygen in the ocean until the end of this century. This might severely affect methane cycling and release from Hydrate Ridge, which is located in the northern outreach of the extensive California continental margin oxygen minimum zone.

[34] **Acknowledgments.** We are grateful for the support of the officers and crew of RV *Sonne* during cruise SO 165-1. Many thanks are owed to Bernhard Bannert, Anja Kähler, Sonja Kriwanek, Birte Mählich, and Wolfgang Queisser for their assistance onboard the ship. Cruise SO 165-1 was supported by the German Federal Ministry of Research and Education (BMBF) as part of the LOTUS project, grants 03G0565A and 03G0565B. This is publication GEOTECH-91 of the program Geotechnologien of BMBF and DFG.

References

Anderson, L. A., and J. L. Sarmiento (1994), Redfield ratios of remineralization determined by nutrient data analysis, *Global Biogeochem. Cycles*, *8*, 65–80.

Barnes, R. O., and E. D. Goldberg (1976), Methane production and consumption in anaerobic sediments, *Geology*, *4*, 297–300.

Boetius, A., and E. Suess (2004), Hydrate Ridge: A natural laboratory for the study of microbial life fueled by methane from near surface gas hydrates, *Chem. Geol.*, *205*(3–4), 291–310.

Boetius, A., K. Ravenschlag, C. J. Schubert, D. Rickert, F. Widdel, A. Gieseke, R. Ammann, B. B. Jørgensen, U. Witte, and O. Pfannkuche (2000), A marine microbial consortium apparently mediating anaerobic oxidation of methane, *Nature*, *407*, 623–626.

Boudreau, B. P. (1996), A method-of-lines code for carbon and nutrient diagenesis in aquatic sediments, *Comput. Geosci.*, *22*(5), 479–496.

Cai, W.-J., and C. E. Reimers (1995), Benthic oxygen flux, bottom water oxygen concentration and core top organic carbon content in the deep northeast Pacific Ocean, *Deep Sea Res.*, *42*, 1681–1699.

Dickens, G. R. (1999), The blast in the past, *Nature*, *401*, 752–753.

Fisher, C. R., I. R. MacDonald, R. Sassen, C. M. Young, S. A. Macko, S. Hourdez, R. S. Carney, S. Joye, and E. McMullin (2000), Methane ice worms: Hesiocaeca methanicola colonising fossil fuel reserves, *Naturwissenschaften*, *87*, 184–187.

Gieskes, J. M., T. Garno, and H. Brumsack (1991), Chemical methods for interstitial water analysis aboard Joides Resolution, *Tech. Note 15*, Ocean Drill. Program, College Station, Tex.

Glud, R. N., J. K. G. Gundersen, and O. Holby (1999), Benthic in situ respiration in the upwelling area off central Chile, *Mar. Ecol. Prog. Ser.*, *186*, 9–18.

Glud, R. N., and N. Blackburn (2002), The effect of chamber size on benthic oxygen uptake measurements: A simulation study, *Ophelia*, *56*, 23–31.

Grasshoff, K., M. Ehrhardt, and K. Kremmling (1983), *Methods of Seawater Analysis*, 419 pp., Verlag Chemie GmbH, Weinheim, Germany.

Greinert, J., G. Bohrmann, and E. Suess (2001), Gas hydrate-associated carbonates and methane-venting at Hydrate Ridge: Classification, distribution, and origin of authigenic lithologies, in *Natural Gas Hydrates: Occurrence, Distribution and Detection*, *Geophys. Monogr. Ser.*, vol. 124, edited by C. K. Paull and W. P. Dillon, pp. 99–113, AGU, Washington, D. C.

Gust, G. (1990), Method of generating precisely-defined wall shearing stresses, Patent 4,973165, U.S. Patent and Trademark Off., Washington, D. C.

Hales, B., and S. Emerson (1997), Evidence in support of first-order dissolution kinetics of calcite in seawater, *Earth. Planet. Sci. Lett.*, *148*, 317–327.

Heeschen, K. U., R. W. Collier, M. A. de Angelis, E. Suess, G. Rehder, P. Linke, and G. P. Klinkhammer (2005), Methane sources, distributions, and fluxes from cold vent sites at Hydrate Ridge, Cascadia Margin, *Global Biogeochem. Cycles*, *19*, GB2016, doi:10.1029/2004GB002266.

Heyer, J. (1990), *Der Kreislauf des Methans*, 250 pp., Akademie, Berlin.

Hinrichs, K. U., and A. Boetius (2002), The anaerobic oxidation of methane: New insights in microbial ecology and biogeochemistry, in *Ocean Margin Systems*, edited by G. Wefer et al., pp. 457–477, Springer, New York.

Hinrichs, K. U., L. R. Hmelo, and S. P. Sylva (2003), Molecular fossil record of elevated methane levels in late Pleistocene coastal waters, *Science*, *299*, 1214–1217.

Hoehler, T. M., M. J. Alperin, D. B. Albert, and C. S. Martens (1994), Field and laboratory studies of methane oxidation in an anoxic marine sediment: Evidence for methanogen-sulphate reducer consortium, *Global Biogeochem. Cycles*, *8*, 451–463.

Ivanenkov, V. N., and Y. I. Lyakhin (1978), Determination of total alkalinity in seawater, in *Methods of Hydrochemical Investigations in the Ocean*, edited by O. K. Bordovsky and V. N. Ivanenkov, pp. 110–114, Nauka, Moscow.

Joos, F., G. K. Plattner, T. F. Stocker, A. Körtzinger, and D. W. R. Wallace (2003), Trends in marine dissolved oxygen: Implications for ocean circulation changes and the carbon budget, *Eos Trans. AGU*, *84*, 197–204.

Kennett, J. P., K. G. Cannariato, I. L. Hendy, and R. J. Behl (2000), Carbon isotope evidence for methane hydrate instability during Quaternary interstadials, *Science*, *288*, 128–133.

Knittel, K., A. Boetius, A. Lembke, H. Eilers, K. Lochte, O. Pfannkuche, P. Linke, and R. Amann (2003), Activity, distribution and diversity of sulfate reducers and other bacteria in sediments above gas hydrate (Cascadia Margin Oregon), *Geomicrobiol. J.*, *20*, 269–294.

Levin, L. A., W. Ziebis, G. F. Mendoza, V. A. Growney, M. D. Tyron, K. M. Brown, C. Mahn, J. M. Gieskes, and A. E. Rathburn (2003), Spatial heterogeneity of macrofauna at northern California methane seeps: Influence of sulfide concentration and fluid flow, *Mar. Ecol. Prog. Ser.*, *265*, 123–139.

Linke, P., E. Suess, M. E. Torres, V. Martens, W. D. Rugh, W. Ziebis, and L. D. Kulm (1994), In situ measurements of fluid flow from cold seeps at active continental margins, *Deep Sea Res., Part I*, *41*, 721–739.

Linke, P., K. Wallmann, E. Suess, C. Hensen, and G. Rehder (2005), In situ benthic fluxes from an intermittently active mud volcano at the Costa Rica convergent margin, *Earth Planet. Sci. Lett.*, *235*, 79–95.

Luff, R., and K. Wallmann (2003), Fluid flow, methane fluxes, carbonate precipitation and biogeochemical turnover in gas hydrate-bearing sediments at Hydrate Ridge, Cascadia margin: Numerical modelling and mass balances, *Geochim. Cosmochim. Acta*, *67*, 3403–3421.

Luff, R., M. Haeckel, and K. Wallmann (2001), Robust and fast FORTRAN and MATLAB libraries to calculate pH distributions in marine systems, *Comput. Geosci.*, *27*, 157–169.

Luff, R., K. Wallmann, and G. Aloisi (2004), Numerical modeling of carbonate crust formation at cold vent sites: Significance for fluid and methane budgets and chemosynthetic biological communities, *Earth Planet. Sci. Lett.*, *221*, 337–353.

MacDonald, I. R., W. W. Sager, and M. B. Peccini (2003), Gas hydrate and chemosynthetic biota in mounded bathymetry at mid-slope hydrocarbon seeps: Northern Gulf of Mexico, *Mar. Geol.*, *198*, 133–158.

Martens, C. S., and R. A. Berner (1977), Interstitial water chemistry of Long Island Sound sediments: I. Dissolved gases, *Limnol. Oceanogr.*, *22*, 10–25.

Milkov, A. V. (2004), Global estimates of hydrate-bound gas in marine sediments: How much is really out there?, *Earth Sci. Rev.*, *66*, 183–197.

Morse, J. W., G. Boland, and G. T. Rowe (1999), A "gilled" benthic chamber for extended measurement of sediment-water fluxes, *Mar. Chem.*, *66*, 225–230.

Olu, K., S. Lance, M. Sibuet, P. Henry, A. Fiala-Médioni, and A. Dinet (1997), Cold seep communities as indicators of fluid expulsion patterns through mud volcanoes seaward of the Barbados accretionary prism, *Deep Sea Res., Part I*, *44*(5), 811–841.

Orphan, V. J., K. U. Hinrichs, W. Ussler III, C. K. Paull, L. T. Taylor, S. P. Syla, J. M. Hayes, and F. F. DeLong (2001a), Comparative analysis of methane oxidizing archea and sulfate-reducing bacteria in anoxic marine sediments, *Appl. Environ. Microbiol.*, *67*(4), 1922–1934.

Orphan, V. J., C. H. House, K. U. Hinrichs, K. D. MCKeegan, and E. F. Delong (2001b), Methane-consuming archea revealed by directly coupled isotopic and phylogenetic analysis, *Science*, *293*, 484–487.

Reeburgh, W. S. (1976), Methane consumption in Cariaco Trench waters and sediments, *Earth Planet. Sci. Lett.*, *28*, 337–344.

Reeburgh, W. S. (1996), "Soft spots" in the global methane budget, in *8th International Symposium on Microbial Growth on C-1 Compounds*, edited by M. E. Lidstrom and F. R. Tabita, pp. 334–342, Springer, New York.

Reeburgh, W. S. (2003), Global methane biogeochemistry, *Treatise Geochem*, *4*, 65–89.

Reeburgh, W. S., S. C. Whalen, and M. J. Alperin (1993), The role of methylotrophy in the global methane budget, in *Microbial Growth on C-1 Compounds*, edited by J. C. Murrell and D. P. Kelly, pp. 1–14, Intercept, Andover, U. K.

Sahling, H., D. Rickert, R. W. Lee, P. Linke, and E. Suess (2002), Macrofaunal community structure and the sulfide flux at gas hydrate deposits from the Cascadia convergent margin, NE Pacific, *Mar. Ecol. Prog. Ser.*, *231*, 121–138.

Schmaljohann, R. (1996), Methane dynamics in the sediment and water column of Kiel Harbour (Baltic Sea), *Mar. Ecol. Prog. Ser.*, *131*, 263–273.

Sommer, S., O. Pfannkuche, D. Rickert, and A. Kähler (2002), Ecological implications of surficial marine gas hydrates for the associated small-sized benthic biota at the Hydrate Ridge (Cascadia Convergent Margin, NE Pacific), *Mar. Ecol. Prog. Ser.*, *243*, 25–38.

Sommer, S., E. Gutzmann, W. Ahlrichs, and O. Pfannkuche (2003), Rotifers colonizing sediments with shallow gas hydrates, *Naturwissenschaften*, *90*, 273–276.

Suess, E., B. Carson, S. D. Ritger, J. C. Moore, M. L. Jones, L. D. Kulm, and G. R. Cochrane (1985), Biological communities at vent sites along the subduction zone off Oregon, *Biol. Soc. Wash. Bull.*, *6*, 475–484.

Suess, E., et al. (1999), Gas hydrate destabilization: Enhanced dewatering, benthic material turnover and large methane plumes at the Cascadia convergent margin, *Earth. Planet. Sci. Lett.*, *170*, 1–15.

Suess, E., et al. (2001), Sea floor methane hydrates at Hydrate Ridge, Cascadia Margin, in *Natural Gas Hydrates: Occurrence, Distribution and Detection*, *Geophys. Monogr. Ser.*, vol. 124, edited by C. K. Paull and W. P. Dillon, pp. 87–98, AGU, Washington, D. C.

Tengberg, A., H. Stahl, G. Gust, V. Müller, U. Arning, H. Anderson, and P. O. J. Hall (2004), Intercalibration of benthic flux chambers: I. Accuracy of flux measurements and influence of chambers hydrodynamics, *Prog. Oceanogr.*, *60*, 1–28.

Thomsen, L., and G. Gust (2000), Sediment stability and characteristics of resuspended aggregates of the western European continental margin, *Deep Sea Res., Part I*, *47*, 1881–1897.

Torres, M. E., J. McManus, D. E. Hammond, M. A. de Angelis, K. U. Heeschen, S. L. Colbert, M. D. Tyron, K. M. Brown, and E. Suess (2002), Fluid and chemical fluxes in and out of sediments hosting methane hydrate deposits on Hydrate ridge, OR, I: Hydrological provinces, *Earth Planet. Sci. Lett.*, *201*, 525–540.

Treude, T., A. Boetius, K. Knittel, K. Wallmann, and B. B. Jørgensen (2003), Anaerobic oxidation of methane above gas hydrates at Hydrate Ridge, NE Pacific Ocean, *Mar. Ecol. Prog. Ser.*, *264*, 1–14.

Tyron, M. D., K. M. Brown, and M. E. Torres (2002), Fluid and chemical flux in and out of sediments hosting methane hydrate deposits on Hydrate Ridge, OR, II: Hydrological processes, *Earth Planet. Sci. Lett.*, *201*, 541–557.

Valentine, D. L. (2002), Biogeochemistry and microbial ecology of methane oxidation in anoxic environments: A review, *Antonie van Leeuwenhoek*, *81*, 271–282.

Valentine, D. L., and W. S. Reeburgh (2000), New perspectives on anaerobic methane oxidation, *Environ. Microbiol.*, *2*, 477–484.

Valentine, D. L., D. C. Blanton, W. S. Reeburgh, and M. Kastner (2001), Water column methane oxidation adjacent to an area of active hydrate dissociation, Eel River Basin, *Geochim. Cosmochim. Acta*, *65*, 2633–2640.

Van Cappellen, P., and Y. Wang (1996), Cycling of iron and manganese in surface sediments: A general theory for the coupled transport and reaction of carbon, oxygen, nitrogen, sulfur, iron, and manganese, *Am. J. Sci.*, *296*, 197–243.

Witte, U., and O. Pfannkuche (2000), High rates of benthic carbon remineralisation in the abyssal Arabian Sea, *Deep Sea Res., Part II*, *47*, 2785–2804.

M. Drews, J. Greinert, P. Linke, O. Pfannkuche, M. Pieper, and S. Sommer, IFM-GEOMAR, Wischhofstraße 1-3, D-24148 Kiel, Germany. (ssommer@ifm-geomar.de)

S. Gubsch, Meerestechnik I, TU Hamburg-Harburg, Schwarzenbergstraße 95, D-21073 Hamburg, Germany.

R. Luff, Bundesamt für Strahlenschutz Messknotennetz Rendsburg, Graf-von-Stauffenberg-Straße 13, D-24768 Rendsburg, Germany.

M. Poser, Institut für Experimentelle und Angewandte Physik, Universität Kiel, Olshausenstraße 40, D-24098 Kiel, Germany.

T. Viergutz, Meerestechnik Bremen GmbH, College Ring 5, IUB Campus, D-28759 Bremen, Germany.